Amazon deforestation: A dangerous future indicated by patterns and trajectories in a hotspot of forest destruction in Brazil

Beatriz Figueiredo Cabral[1], Aurora Miho Yanai[1], Paulo Maurício Lima de Alencastro Graça[1], Maria Isabel Sobral Escada[2], Cláudia Maria de Almeida[2], Philip Martin Fearnside[1]

[1] Instituto Nacional de Pesquisas da Amazônia (INPA), Av. André Araújo n° 2936, CEP 69067-375, Manaus, Amazonas, Brazil, beatriz.figueiredocabral@gmail.com; yanai@inpa.gov.br pmlag@inpa.gov.br; pmfearn@inpa.gov.br
[2] Instituto Nacional de Pesquisas Espaciais (INPE), Av. dos Astronautas, 1758, CEP 12227-010, São José dos Campos, São Paulo, Brazil, isabel.escada@inpe.br; claudia.almeida@inpe.br

ABSTRACT

In recent years, the loss of forest in the Brazilian Amazon has taken on alarming proportions, with 2021 recording the largest increase in 13 years, particularly in the Abunã-Madeira Sustainable Development Reserve (SDR). This has significant environmental, social, and economic repercussions globally and for the local communities reliant on the forest. Analyzing deforestation patterns and trends aids in comprehending the dynamics of occupation and deforestation within a critical Amazon region, enabling the inference of potential occupation pathways. This understanding is crucial for identifying deforestation expansion zones and shaping public policies to curb deforestation. Decisions by the Brazilian government regarding landscape management will have profound environmental implications. We conducted an analysis of deforestation patterns and trends up to 2021 in the municipality (county) of Lábrea, located in the southern portion of Amazonas state. Deforestation processes in this area are likely to spread to the adjacent "Trans-Purus" region in western Amazonas, where Amazonia's largest block of remaining rainforest is at risk from planned highways. Annual deforestation polygons from 2008 to 2021 were categorized based on occupation typologies linked to various actors and processes defined for the region (e.g., diffuse, linear, fishbone, geometric, multidirectional, and consolidated). These patterns were represented through 10×10 km grid cells. The findings revealed that Lábrea's territory is predominantly characterized by the diffuse pattern (initial occupation stage), mainly concentrated in protected areas. Advanced occupation patterns (multidirectional and consolidated) were the primary contributors to deforestation during this period. Observed change trajectories included consolidation (30.8%) and expansion (19.6%) in the southern portion of the municipality, particularly along the Boi and Jequitibá secondary roads, providing access to large illegal landholdings. Additionally, non-change trajectories (67%) featured initial occupation patterns near rivers and in protected areas, likely linked to riverine and extractive communities. Tailoring measures to control deforestation based on actor types and considering stages of occupation is crucial. The techniques developed in this study provide a comprehensive approach for Amazonia and other tropical regions.

Keywords – deforestation actors; occupation typologies; cattle-ranching Amazon frontier; land-use change; land grabbing

1. Introduction

1.1. Amazon deforestation's consequences for Brazil and the world

The central role of Amazon deforestation in the global climate and biodiversity crises, as well as its environmental and social impacts in the Amazon region, have made the containment of this destruction a top priority for both the world and for the Amazonian countries (Fearnside, 2021a). With over 40% of the world's remaining tropical forests, Brazil is by far the most important country in terms of potential impacts of tropical deforestation and degradation on global climate (Laurance et al., 2001). This stems not only from the substantial year-to-year carbon emission, but also from the potential emissions of the huge carbon stocks in the remaining forest biomass and in the soil under the forest if released by forest degradation from increasing temperatures, drought severity and forest fires linked to climate change (Barros and Fearnside, 2019; Nogueira et al., 2015). Release of this carbon over a span of a few years would be a key factor in pushing global climate past a tipping point beyond which human countermeasures by cutting emissions would be incapable of stopping the further advance of global warming driven by positive feedbacks in the Earth system (Fearnside, 2022).

The municipality (county) of Lábrea, the focus of our study, is located in the southern portion of Brazil's state of Amazonas and is adjacent to the Trans-Purus region, a vast area that has largely remained undisturbed due to the lack of accessibility by roads. The Trans-Purus region, located in the western portion of the state of Amazonas, has an extensive area of "undesignated public forests," a term referring to government land that has not been assigned to a specific use such as a conservation unit (a protected area for biodiversity), an Indigenous land or a settlement project. These undesignated public forests are the most attractive areas for illegal land occupation by land grabbers, organized landless farmers, loggers, and other groups. The occupation processes occurring in Lábrea are likely to expand to the Trans-Purus region (Fearnside, 2017, 2018; Fearnside et al., 2020). The Trans-Purus region faces deforestation risks from roads planned to branch off the BR-319 (Manaus-Porto Velho) highway. BR-319 highway was initially built in 1972-1973 and abandoned in 1988; it received "maintenance" beginning in 2015 and is now slated for "reconstruction," pending environmental license approval (Figure 1) (Fearnside, 2022; Santos et al., 2023).

If the forest in the Trans-Purus region is lost it would be catastrophic for Brazil, since this area is crucial for recycling the water that is transported to São Paulo and other parts of southeastern and southern Brazil via the winds known as "flying rivers" (Fearnside, 2004, 2015). The prevailing winds in Amazonia blow from east to west because of the effect of the Earth's rotation on the return flow of the Hadley circulation, and these winds bring water that has evaporated from the Atlantic Ocean. Roughly half of the water that falls as rain over Amazon forest is recycled by the trees, which release it as water vapor that, along with the remaining water vapor derived directly from the Atlantic, is carried further by winds (Zemp et al., 2014). South American low-level jet winds are blocked by the Andes mountains and turn to the south and east, transporting water vapor to São Paulo, other parts of southeast and southern Brazil and to neighboring countries (Nicolini et al., 2002; Arraut et al., 2012). This transport is especially strong during December, January and February when the intertropical convergence zone is at its southernmost position and the winds meet the highest part of the Andes. This is rainy season in southeastern South America and is the critical period when the reservoirs that supply the city of São Paulo fill, as well as the many other reservoirs in southeastern and southern Brazil and in neighboring countries. The La Plata River basin, which includes São Paulo, depends on water vapor from Amazonia

for 70% of its annual precipitation (van der Ent et al., 2010). A catastrophic drought in 2014 brought São Paulo, the fourth largest city in the world, close to running out of water even for drinking (Nobre et al., 2016; Cunha et al., 2019; Fearnside, 2021b). In 2021 another catastrophic drought struck this part of Brazil (Fernandes et al., 2021; Getirana et al., 2021). These droughts result from changes in ocean temperatures linked to global warming, and they are expected to intensify with projected climate change (Biastoch and Boning, 2013; Coelho et al., 2016). These changes increase the value of maintaining Amazon forest, especially in the Trans-Purus region, as there is no longer any leeway to allow loss of water transported by the "flying rivers."

1.2. Amazon deforestation and the Lábrea hotspot

From 2019 to 2021, annual deforestation in the Amazon biome in Brazil increased by 56.6% when compared to the years from 2016 to 2018, surpassing 10,000 km² per year (INPE, 2021; Alencar et al., 2022). In 2021, the state of Amazonas jumped to second place in the ranking for annual deforestation among the nine states in Brazil's Legal Amazon region (an area the size of western Europe), taking over the historical position previously occupied by Mato Grosso and remaining behind only the state of Pará (InfoAmazonia, 2021).

In recent years, deforestation has been concentrated mainly in eastern Acre, northern Rondônia, and southern Amazonas, which make up the AMACRO integration zone, or the recently renamed Abunã-Madeira Sustainable Development Zone. AMACRO was created in 2021 during the 2019-2022 presidential administration of Jair Bolsonaro with the justification of promoting environmental sustainability through the economic development of the 32 municipalities that make up this region (SUDAM, 2021). However, the prospect of replacing the existing local economy with an agribusiness-based economy aimed at exporting commodities is tied to the intensification of rural violence, as observed in this area (CPT, 2021; IPAM, 2021; IMAZON, 2022). As the potential for large-scale soy plantations and ranching operations increases, there is heightened demand for land and an escalation of land conflicts. These conflicts often manifest as "land grabbing," a term specific to Amazonia, denoting the large-scale, illegal claiming of land, typically on government-owned territories (different from the same term's meaning in Africa and Asia, where it refers to foreign groups purchasing local land) (Agrawal et al., 2019). Government land is invaded both by land grabbers and by small farmers (both organized and individual). The result has been increased deforestation rates (IMAZON, 2022). The occupation process in Lábrea reflects a historical context marked by intense land conflicts related to illegal and disorderly occupation, expansion of cattle ranching, predatory fishing and hunting, illegal logging, and landholdings in protected areas (Tavares and Cordeiro, 2017; CPT, 2021). The term "landholdings" used here refers to self-declared claims in the Rural Environmental Registry (CAR) and does not imply that claimants have ownership or legal title to the areas.

1.3. Typology of deforestation patterns in the Amazon

Addressing escalating deforestation and its profound consequences for humanity is crucial, prompting the need for a comprehensive understanding of this dynamic process. Given the intricate connection between deforestation and changes in land use, it is crucial to comprehend and link the actors and factors involved, forming the basis for targeted policies to mitigate the negative impacts of deforestation on the environment and society (Marinaro et al., 2022). To achieve a thorough understanding of land occupation, a robust approach involves discerning the typology of deforestation patterns and correlating them with actors and different stages of occupation in a region (McGarigal and Marks, 1995; Mertens and Lambin, 1997; Pereira et al., 2007; Silva et

148 al., 2008). This correlation could allow inferences about the evolutionary stage of the
149 occupation and deforestation process in a given area, including likely occupation
150 trajectories (Diniz, 2002; Oliveira and Metzger, 2006; Gavlak et al., 2011).
151   Previous studies in the Amazon have successfully employed typologies to
152 categorize deforestation patterns, shedding light on the characteristics associated with
153 various stages of occupation. For instance, Silva et al. (2008) identified distinct patterns
154 such as linear, small isolated irregular, small irregular near roads, medium irregular near
155 roads, and large geometric, each linked to specific actors and landholding
156 characteristics. Saito et al. (2011) classified deforestation based on occupation stages,
157 distinguishing between consolidated, diffuse, fishbone, regular geometric,
158 multidirectional disordered, and unidirectional linear patterns. Similarly, Gavlak et al.
159 (2011) defined deforestation patterns and trajectories along a specific highway,
160 providing insights into stages of occupation and associated changes. In a different study,
161 Marinaro et al. (2022) defined the stages and actors of deforestation in a livestock
162 frontier in the Dry Chaco of northern Argentina, contributing to the understanding,
163 organization, and differentiation of various social-ecological processes and perceptions
164 from local-urban inhabitants.
165   Building upon these insights, the region containing the municipality of Lábrea
166 presents an emergent scenario influenced by a cattle-ranching frontier, consolidating its
167 significance as an important area for comprehending land-occupation dynamics. To gain
168 insight into the recent dynamics of deforestation in the municipality of Lábrea, this
169 study endeavors to understand the patterns and trajectories of land occupation in the
170 region. Focusing on identifying deforestation patterns and trajectories in the
171 municipality of Lábrea from 2008 to 2021 will contribute valuable knowledge to inform
172 policies aimed at mitigating deforestation rates in this critical region.

173 **2. Materials and methods**

174 2.1. *Study Area*

175   The present study was carried out in the municipality of Lábrea, located in the
176 southern mesoregion of the state of Amazonas near the borders with the states of
177 Rondônia and Acre (Figure 1). The main rivers in the municipality are the Ituxi and
178 Purus, with the Purus River being used as the access route to the municipal seat (the city
179 of Lábrea; 2021 urban population = 24,223) (Tavares and Cordeiro, 2017; IBGE,
180 2021a). In addition to the river, it is also possible to access the city of Lábrea by the
181 BR-230 (Transamazon) highway, and the southern portion of the municipality can be
182 accessed by secondary roads branching off the BR-364 (Porto Velho-Rio Branco)
183 highway; these secondary roads, built illegally by landgrabbers, have played an
184 important role in the process of occupying this area (Franco, 2011; Tavares and
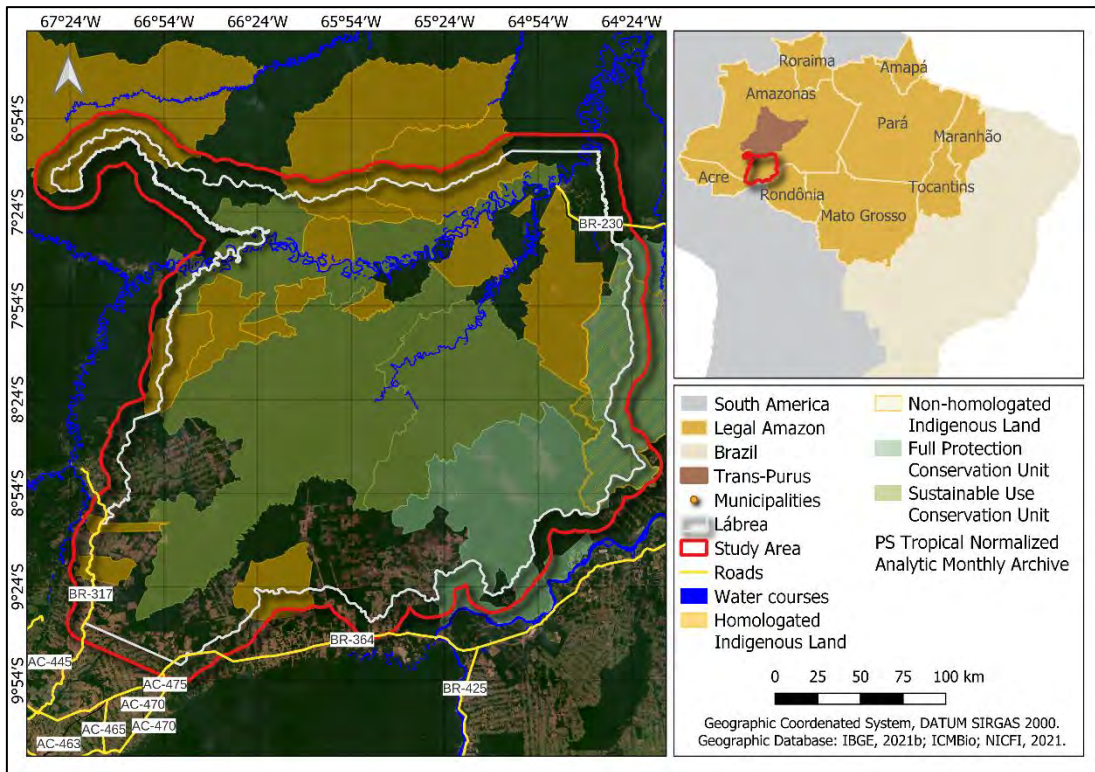185 Cordeiro, 2017).

Figure 1. Location map of study area, municipality of Lábrea, Amazonas state.

The study area encompasses 83,900 km² (an area larger than Austria or the Brazilian state of Paraíba). The study area includes a 10-km buffer surrounding the municipality of Lábrea. The buffer was delineated to avoid possible information losses regarding deforestation patterns caused by the neighborhood of the municipality. Around 80% of the study area is in protected areas, divided into 17 Indigenous lands and four conservation units. The vegetation cover in Lábrea is predominantly composed of dense ombrophilous lowland forest (RADAMBRASIL, 1978). The soils are classified as Latosols, Argisols, Plinthosols, and, in areas near the rivers, Gleysols (IBGE, 2020). The relief is formed by depressions and plains, with altitudes ranging from 38 m to 1089 m above mean sea level. The climate is characterized as tropical monsoon (Type Am-i in the Köppen classification system), with short dry periods and a long period with high precipitation (2400 to 2800 mm year [1]) (Alvares et al., 2013).

2.2. *Deforestation mapping and definition of occupation typology*

Cumulative deforestation data for 2008, 2013, 2017, and 2021 were obtained from the Project for Monitoring Deforestation in the Legal Amazon by Satellite (PRODES) vector maps (INPE, 2021). The selection of these specific years aimed to analyze the distinct occupation patterns during periods with varying occupation dynamics. PRODES, at the National Institute for Space Research (INPE), estimates annual rates of deforestation by clearcutting based on visual interpretation of satellite images and provides extensive spatial data through the TerraBrasilis digital platform (Assis et al., 2019; INPE, 2021). Widely recognized for its accuracy, PRODES boasts a precision level of 93.5%, establishing its reputation as a reliable deforestation monitoring system (Maurano et al., 2019).
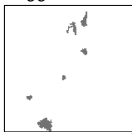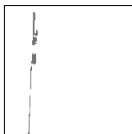
The analysis of deforestation patterns and trajectories using PRODES data proves invaluable in indicating and characterizing diverse processes of forest-cover change associated with agents and types of occupation, enabling a comprehensive

216 understanding of the deforestation and the occupation processes involved. This
217 approach involves creating a typology that establishes and describes the connection
218 between the spatial deforestation patterns in the analyzed area and their semantics.
219 Auxiliary information, such as agribusiness census data, and field information are used
220 in this process. Through exploratory spatial analysis of the arrangement and shape of
221 deforestation polygons and patterns described in the literature, an occupation typology
222 was defined for the Lábrea region based on Azeredo et al. (2016), Gavlak et al. (2011),
223 Saito et al. (2011), and Yanai et al. (2020). The identification and definition of these
224 patterns were also informed by an expedition carried out in the study area in October
225 2021, revealing different occupation dynamics.
226   After defining the typology of occupation patterns, the deforestation polygons
227 were analyzed in the context of individual cells. This process involved examining the
228 landscape metrics of the polygons within predetermined cell sizes. Previous studies
229 suggest that the choice of the grid-cell size should consider the dimensions of
230 deforestation patches and their spatial distribution to avoid loss of information or
231 distortion of patterns (Saito, 2010; Gavlak et al., 2011; Saito et al., 2012; Pinheiro et al.,
232 2016; Assis et al., 2021). After preliminary tests and an empirical analysis of the
233 arrangement of deforestation patterns when displayed with different cell sizes, it was
234 found that 10 × 10 km was the most suitable cell size for identifying and describing the
235 patterns proposed in Table 1. Cells where no deforestation patches were observed were
236 classified as "forest."
237

238
239
240 **Table 1.** Typology of deforestation patterns associated with human occupation in the
241 municipality of Lábrea (white = forest, gray = deforestation).

Deforestation Pattern	Description
Diffuse	Small, isolated patches with low to medium density, evenly distributed. This is characteristic of the initial spontaneous occupation distributed along riverbanks, in mining areas, and where small landholders are located.
Linear	Elongated, continuous patches. This is related to the initial occupation distributed along roads.
Geometric	Small and medium patches with regular geometry. This represents an initial to intermediate stage of occupation by medium and large landholders.
Fishbone	Long, branching patches along roads, with an appearance similar to the skeleton of a fish. They represent an intermediate stage of occupation by small and medium landholders, as well as areas intended for settlement projects.
Multidirectional	Large and medium-sized multidirectional patches with irregular geometry. They represent an intermediate to advanced stage of disorderly occupation.
Consolidated	Large areas with undefined shape. They have a high density of deforestation with few or almost no forest fragments.

242 2.3. *Classification of deforestation patterns and trajectories*
243   Deforestation patterns were classified using spatial data-mining techniques. This
244 procedure was performed using the Geographical Data Mining Analyst (GeoDMA)
245 plugin, a classifier developed by Körting et al. (2008) for TerraView version 5.6.1
246 software. It combines a set of tools for integrating and analyzing remote-sensing images
247 with data-mining techniques for extracting information and discovering knowledge
248 about large databases (INPE, 2020). This tool allows for the structural classification of
249 objects by extracting a set of landscape metrics that measure and describe the
250 occupation patterns.
251   The classification process conducted by GeoDMA involved the following steps:
252 1) extraction of landscape metrics from deforestation polygons within 10 × 10-km cells;
253 2) compilation of a comprehensive set of training samples for the deforestation class; 3)
254 application of the C5.0 decision tree algorithm to classify and validate the deforestation

255 patterns (Quinlan, 2017), and 4) evaluation of the classification results by analyzing the
256 confusion matrix generated for the training samples.
257   During the training phase, a single set of samples was constructed for the four
258 analyzed years (i.e., 2008, 2013, 2017, and 2021). This allowed for patterns that are not
259 present in a given year to be included in another period, composing a unique typology
260 that considered deforestation patterns for all years. In total, 383 training samples were
261 collected, of which 60 samples corresponded to diffuse, forest, and geometric patterns,
262 58 samples were collected for the multidirectional pattern, 55 samples for the
263 consolidated pattern, and 45 samples for the fishbone and linear patterns. Due to the low
264 frequency of some deforestation patterns in the study area, such as the linear and
265 fishbone patterns, different numbers of samples were selected for each class.
266   Once the training samples were collected, we used the C5.0 algorithm with its
267 "boosting" feature, which generates a predefined number of trees where the final
268 classification of each segment is the one that was assigned by the majority of the
269 decision trees (Quinlan, 2017). GeoDMA automatically separated 66% (254 samples) of
270 the collected samples to classify the patterns (i.e., decision-tree generation), and 34%
271 (129 samples) for validation.
272   As a result of using the boosting tool, a predetermined set of 30 decision trees
273 was generated, where the categorical attributes (i.e., deforestation patterns) were
274 classified from the non-categorical attributes (i.e., values of landscape metrics). In total,
275 17 landscape metrics were used, of which three were in over 90% of the classifications,
276 namely: Class Area (CA), Landscape Shape Index (LSI), and Patch Richness (PR). The
277 following metrics also had a certain degree of importance (i.e., utilization values above
278 60%): Area-Weighted Mean Patch Fractal Dimension (AWMPFD), Total Area of the
279 Biggest Object (TABO), Patch Density (PD), Biggest Intersection Area (BIA), and
280 Area-Weighted Mean Shape Index (AWMSI). These metrics, by quantifying the spatial
281 structure and composition of landscapes, provide insights into the characteristics of
282 deforestation polygons in the grid, facilitating the identification of patterns, changes,
283 and trends over time. For a comprehensive understanding of these metrics, refer to the
284 Supplementary Material (Table S.1).
285   In the final step, two confusion matrices were generated to evaluate the result of
286 combining decision trees regarding the classification of training and validation samples
287 (Table 2). For the evaluation samples the total accuracy was 92% and the Kappa
288 coefficient was 91%, these values being in the range considered to be quite satisfactory
289 (Hudson and Ramm, 1987).
290

Table 2. Confusion matrix of validation samples used in the classification of deforestation patterns for the study area for the four analyzed years (2008, 2013, 2017, and 2021) *

	CON.	DI.	FISH.	FO.	GE.	LI.	MUL.	P (%)
CON.	14							100
DI.		20				3		87
FISH.			15				1	94
FO.				20				100
GE.					24		1	96
LI.		1	2		1	13		76
MUL.			1				13	93
U (%)	100	95	83	100	96	81	87	
OA								**0.92**

* The analyses use 129 validation samples. Con.= Consolidated; Dif. = Diffuse; Fish. = Fishbone; Fo. = Forest; Ge. = Geometric; Li. = Linear; Mul. = Multidirectional; P = Producer's Accuracy; U = User's Accuracy; OA: = Overall Accuracy.

Deforestation trajectories between 2008 and 2021 were obtained from the results of the pattern classification. These trajectories were divided into "changing" and "non-changing," as proposed by Gavlak (2011). Change in trajectories refers to cells whose patterns were altered over the years, divided into "expansion" and "consolidated." The "expansion" trajectory is characterized by the cells initially having no deforestation (i.e., they were forest), but in the following years they were classified with patterns with initial to intermediate deforestation levels (i.e., diffuse, linear, geometric and fishbone). "Consolidation" is represented by all cells that in the first year presented an initial or intermediate occupation and by the last year had advanced to a multidirectional or a consolidated pattern (Figure 2). Cells that maintained the same pattern as in 2008 in the final year were classified as one of the "non-changing" trajectories according to the observed deforestation pattern, namely: diffuse, consolidated, and "others" (which encompasses the multidirectional, fishbone, geometric and linear patterns).
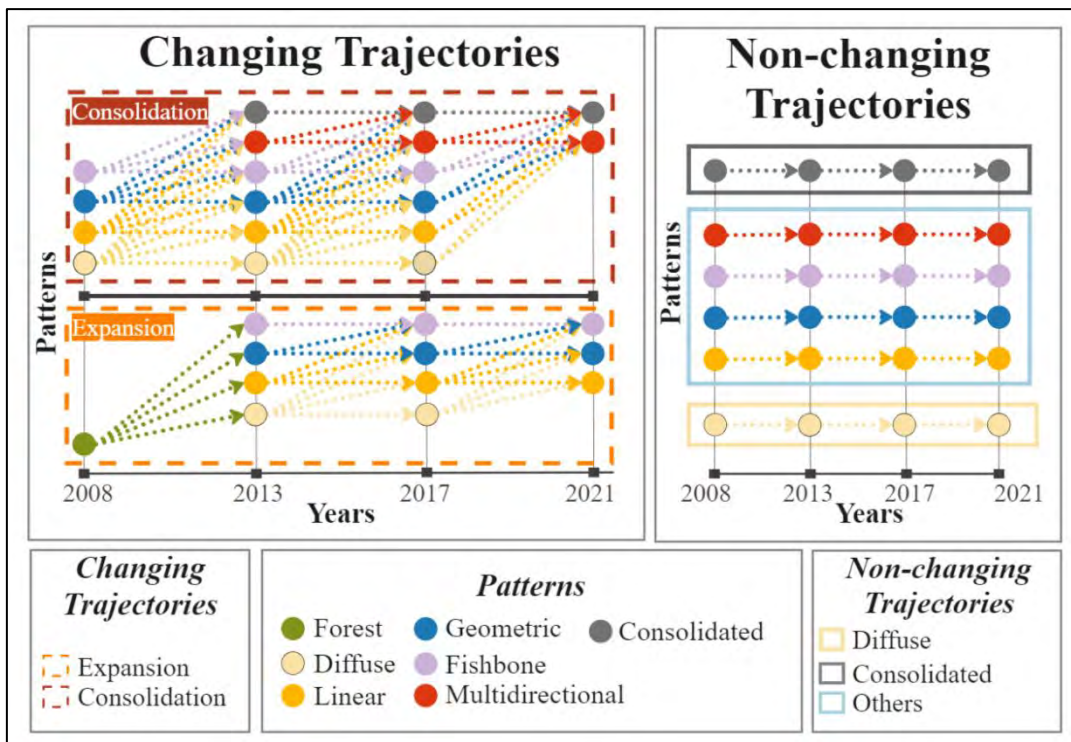
Figure 2. Trajectories of change: consolidation and expansion, and non-changing
trajectories: diffuse, consolidated and others (Adapted from Gavlak, 2011).

These trajectories were obtained both for change between the initial and final
maps (i.e., from 2008 to 2021), and in the three-time intervals between 2008 and 2021
(i.e., from 2008 to 2013, from 2013 to 2017, and from 2017 to 2021). The first analysis
made it possible to capture the differences in patterns for the entire period from 2008 to
2021, resulting in a single final map of occupation trajectories, while the second
allowed understanding the evolution of trajectories over the periods analyzed.
In this study the dataset does not allow for the identification of areas that have
reverted to forest once classified as deforested. This limitation reflects the relatively
short time frame of the analysis, which is insufficient to observe complete forest
regeneration.

2. Results

3.1. *Deforestation patterns*
The evolution of deforestation patterns from 2008 to 2021 is presented in the
maps in Figure 3. In general, it is possible to observe that the diffuse pattern (i.e., initial
occupation) was predominant and concentrated mostly in areas near rivers and in areas
that may indicate new deforestation fronts. Although the deforested area in cells
classified as diffuse increased over the years, from 12.7 to 14.6 thousand hectares from
2008 to 2021, as exemplified in Table 3, this amount observed in 2021 represented only
1.5% of the total deforested area, considering all patterns (Figure 4).
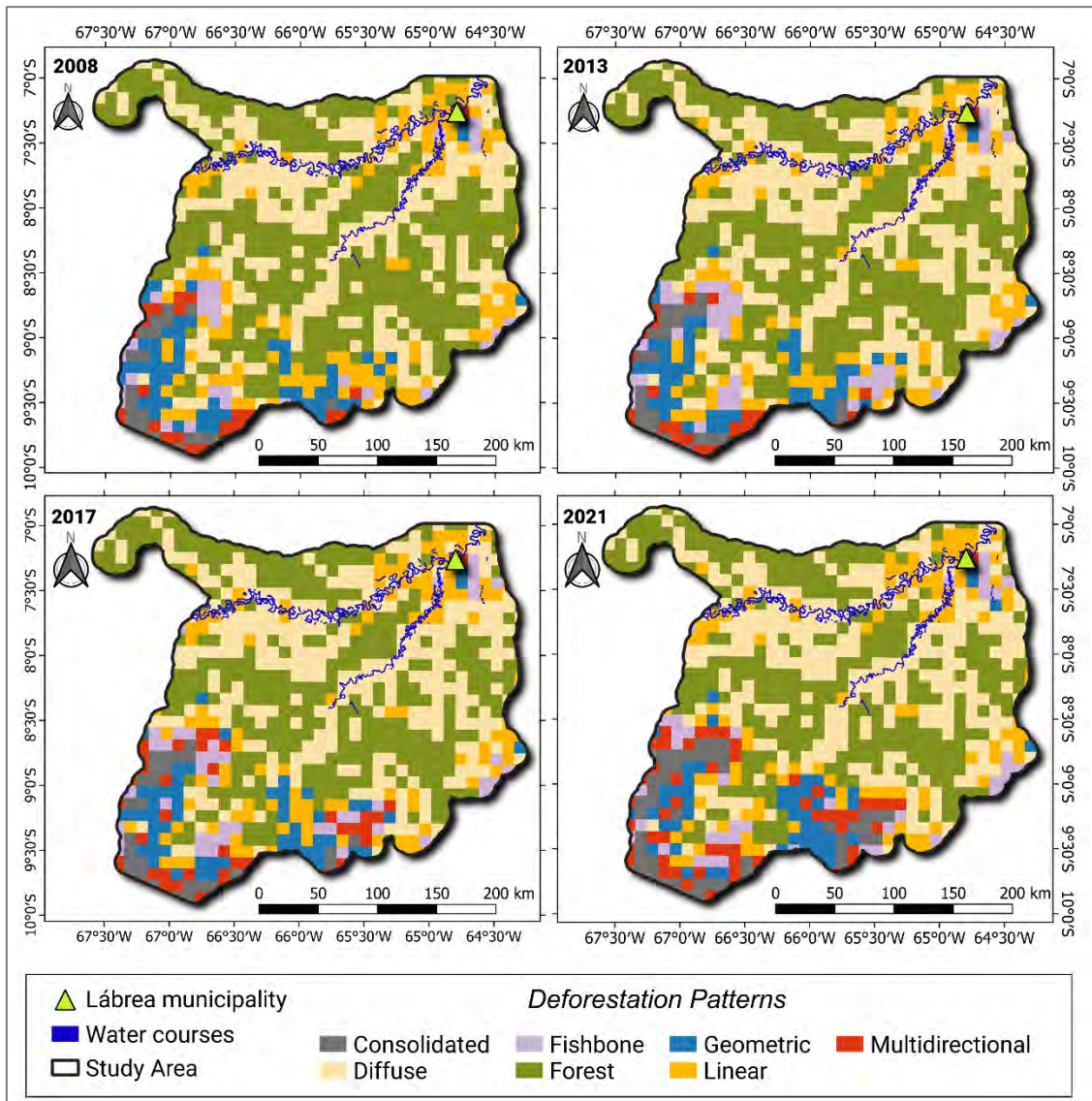
Figure 3. Classification maps of occupancy patterns for the years 2008, 2013, 2017, and 2021 for the study area (i.e., municipality of Lábrea + 10-km buffer).
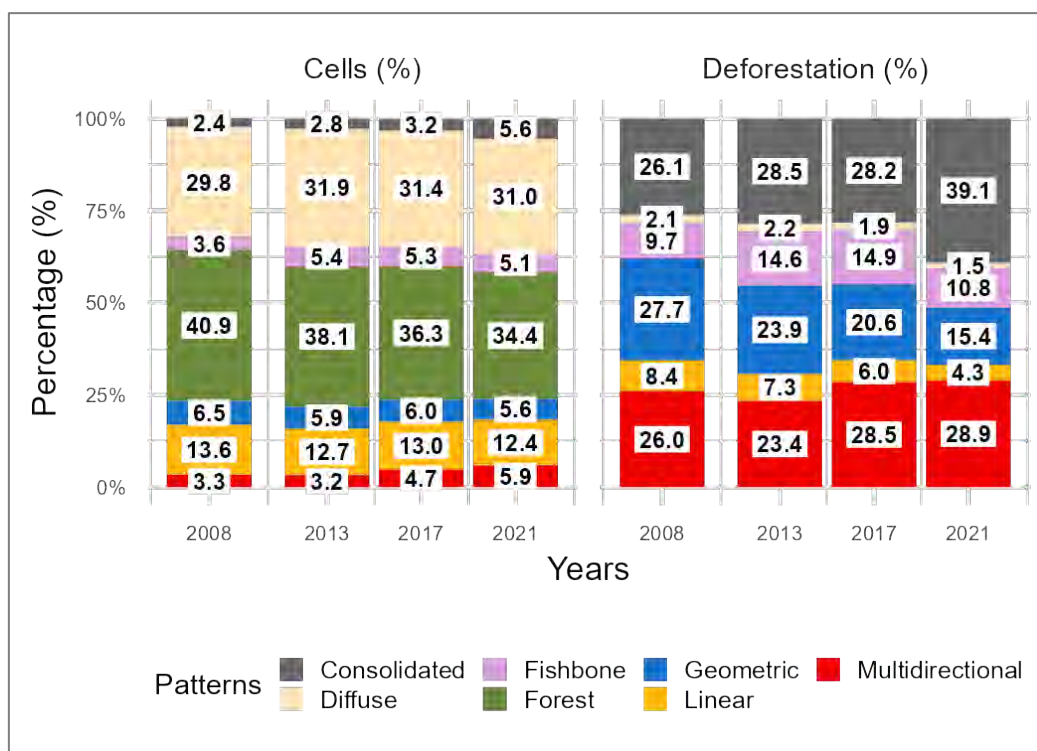
Figure 4. Evolution of the quantities of classified cells (%) and proportion of cumulative deforested area (%) for each type of deforestation pattern for the years 2008, 2013, 2017, and 2021.

Table 3. Evolution of cumulative deforested area, in hectares, for each deforestation pattern in the study area in 2008, 2013, 2017, and 2021.

Deforestation patterns	Cumulative deforested area (ha)			
	2008	*2013*	*2017*	*2021*
Consolidated	157,806.70	187,416.65	219,142.62	382,057.48
Diffuse	12,711.50	14,539.63	14,519.02	14,640.14
Fishbone	58,620.54	95,940.64	115,762.75	105,107.86
Geometric	167,178.21	157,325.14	159,579.75	150,823.57
Linear	50,554.12	48,251.45	46,211.81	41,737.13
Multidirectional	156,867.13	153,508.96	221,137.62	282,859.86
Total	603,738.19	656,982.46	776,353.58	977,226.04

The multidirectional and consolidated patterns, which represent advanced stages of occupation, occurred mainly in the southern portion of the municipality of Lábrea. Although these patterns had lower percentages of cells compared to the diffuse pattern, they together represented 52.1%, 51.9%, 56.7%, and 68.0% of the deforested area for the years 2008, 2013, 2017, and 2021, respectively (Figures 3 and 4). An analysis of the deforested areas within these cells revealed a greater percentage increase in deforestation for the consolidated pattern between 2017 and 2021. Over the course of four years, the deforested area in consolidated cells increased by 162.9 thousand hectares, whereas the multidirectional pattern showed an increase of only 61.7 thousand hectares during the same period, and 67.6 thousand hectares from 2013 to 2017 (Table 3).

The linear and geometric patterns showed similar dynamics over the years regarding the number of cells, with a reduction in area when comparing the years 2008 and 2021, reflecting a gradual reduction in cells classified as linear and geometric (Figure 4). Since these patterns are related to the initial and intermediate stages of occupation, respectively, the increase in deforested area in the cells implies a transition to patterns in more advanced stages. Thus, over the years, a linear pattern cell changed to the geometric or fishbone pattern, and the geometric pattern, in turn, progressed to the multidirectional or consolidated pattern. Note that the fishbone pattern showed a significant increase from 2008 to 2017.

3.2. *Temporal evolution of deforestation trajectories*

The temporal evolution of trajectories during the three intervals between 2008 and 2021 (i.e., from 2008 to 2013, from 2013 to 2017, and from 2017 to 2021) are illustrated in Figure S1. The change trajectories (i.e., "consolidation" and "expansion") and the "consolidated" no-change trajectory (i.e., cells that maintained the consolidated pattern) presented similar frequencies with a slight increase over the years for the consolidation and expansion trajectories but remained lower than the number of cells with the diffuse and "others" trajectories (i.e., cells that maintained fishbone, linear, or multidirectional patterns in the analyzed periods).

Both cells with the "consolidation" trajectory and cells with the "expansion" trajectory showed increases in deforestation, and the cumulative deforested areas in both classes increased over the years (Table 4). However, the contribution to deforestation in Lábrea from areas undergoing consolidation was higher than in the expansion areas for all three periods. The greatest increase in deforested area for both trajectories ("consolidation" and "expansion") occurred between the last two periods (i.e., between 2013 and 2017, and 2017 and 2021), with the cumulative deforestation from consolidation increasing 2.7 times between 2013 and 2017, and 2.4 times from 2017 to 2021. The expansion trajectory had growth similar to these between 2013 and 2017 (increasing 2 times) and from 2017 to 2021 (increasing 1.6 times). This indicates that the speed at which areas are undergoing consolidation is similar to areas undergoing expansion.

390
391 **Table 4.** Evolution of the cumulative deforested area, in hectares, for each deforestation
392 trajectory and for the patterns that compose the "others" trajectories in the study area in
393 the years 2013, 2017 and 2021.

| Deforestation trajectory	Cumulative deforested area (ha)			Deforested area (%)		
	2013	*2017*	*2021*	*2013*	*2017*	*2021*
Consolidation	39,295.58	107,891.84	264,575.66	6.0%	13.9%	27.1%
Expansion	19,053.60	37,977.85	60,841.33	2.9%	4.9%	6.2%
Consolidated	160,245.84	192,254.68	229,299.02	24.4%	24.8%	23.5%
Diffuse	13,581.70	13,900.60	14,355.63	2.1%	1.8%	1.5%
Others						
Fishbone	82,004.08	95,643.96	90,573.58	-	-	-
Geometric	154,571.61	149,130.81	116,948.83	-	-	-
Linear	46,845.87	39,420.12	38,084.78	-	-	-
Multidirectional	141,384.17	140,133.72	162,547.21	-	-	-
Subtotal	424,805.73	424,328.62	408,154.40	64.6%	54.6%	41.7%
TOTAL	**656,982.46**	**776,353.58**	**977,226.04**	**100%**	**100%**	**100%**

394   The non-changing trajectories classified as diffuse and "others" showed similar
395 behaviors in relation to cell frequency and the percentage of deforestation, decreasing
396 from the initial value of 64.6% in 2013 to 41.7% in 2021 (Table 4). However, the
397 relationship between the proportion of cells and the proportion of deforestation differed
398 between these classes. Cells with the "others" trajectory accounted for the most
399 deforestation in Lábrea (Table 4).
400   The frequencies of patterns with their respective proportions of deforestation in
401 cells classified in the "others" trajectory (i.e., proportion of non-change in the fishbone,
402 geometric, linear and multidirectional patterns) are given in Figure 5. The geometric and
403 multidirectional patterns had the highest contributions to the observed deforestation in
404 this trajectory, so that the geometric pattern decreased while the percentage of cells and
405 deforested area in the multidirectional pattern increased. This may indicate that
406 deforestation increased in cells with the geometric pattern, causing them to no longer be
407 part of the non-changing trajectory and changing to patterns of deforestation in more-
408 advanced stages of occupation (i.e., there was an increase of deforestation in cells with
409 geometric patterns that changed to multidirectional or consolidated patterns, noting that
410 in the next analyzed period there was a smaller number of cells with the geometric
411 pattern and a lower percentage of the deforestation represented by them).

412
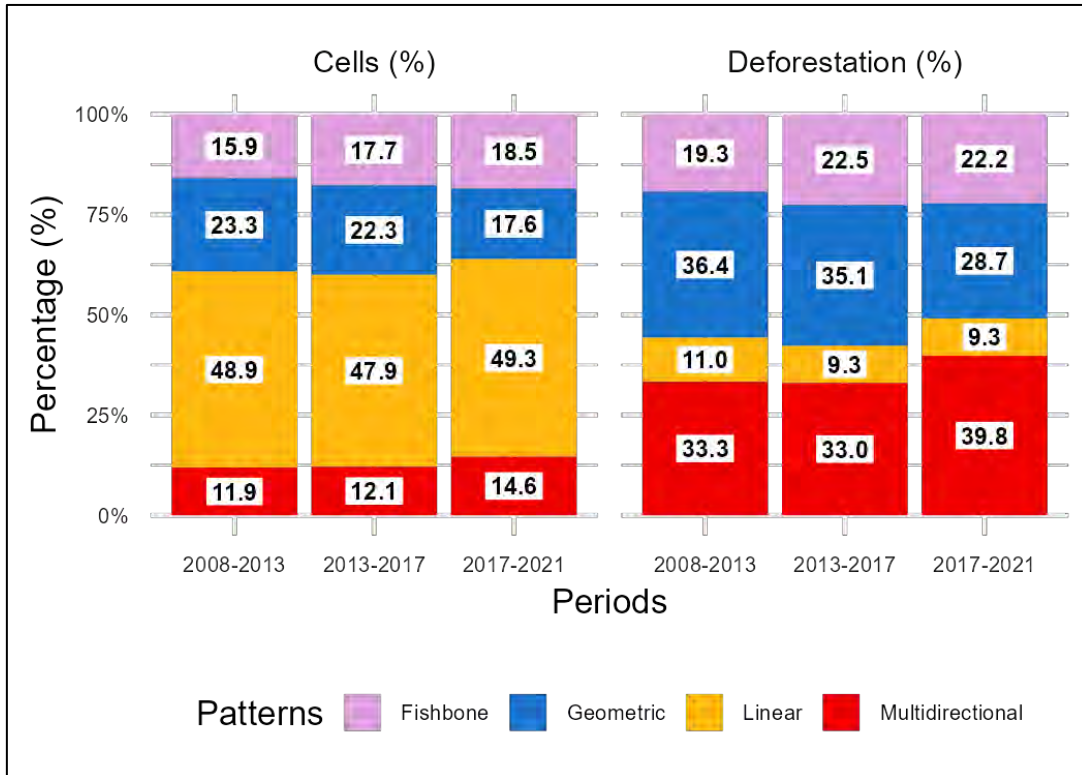
413
414 **Figure 5.** Evolution of the occupation patterns that make up the non-change trajectories
415 (i.e., "others") in the study area in the periods from 2008 to 2013, 2013 to 2017, and
416 2017 to 2021.
417
418   For the linear and fishbone patterns, the proportions of deforested area varied
419 from 9.3 to 22.5%, with distinct dynamics over time (Figure 5). An increase in
420 deforested area was observed for the fishbone pattern, representing 22.2% of the total
421 deforested area in the last period, which corresponds to 90.6 thousand hectares (Table
422 4). Cells that maintained the linear pattern, despite having a higher frequency than the
423 previous pattern, had a reduction in deforested area over the years (Table 4). Both
424 patterns are mainly related to early and intermediate stages of occupation, with changes
425 to more advanced patterns being frequent over the years.
426
427 *3.2. Deforestation trajectories*
428   The final trajectory of deforestation for Lábrea (i.e., between the years 2008 and
429 2021), obtained from the analysis of pattern changes in different stages of occupation, is
430 represented in Figure 6. Cells that presented change trajectories (i.e., "consolidation"
431 and "expansion") are mainly located in the southern portion of Lábrea, and, despite their
432 low frequency compared to the others (29.4%), they represented 50.4% of deforestation
433 in 2021 (Table S.2 in Supplementary material). The deforested area in cells undergoing
434 consolidation and expansion is equivalent to 302,000 and 190,000 ha, respectively.
435 Cells in expansion near rivers and in non-change trajectories with the diffuse pattern are
436 mainly related to early occupations, as observed in Figures 3 and 4, and have smaller
437 deforested areas.
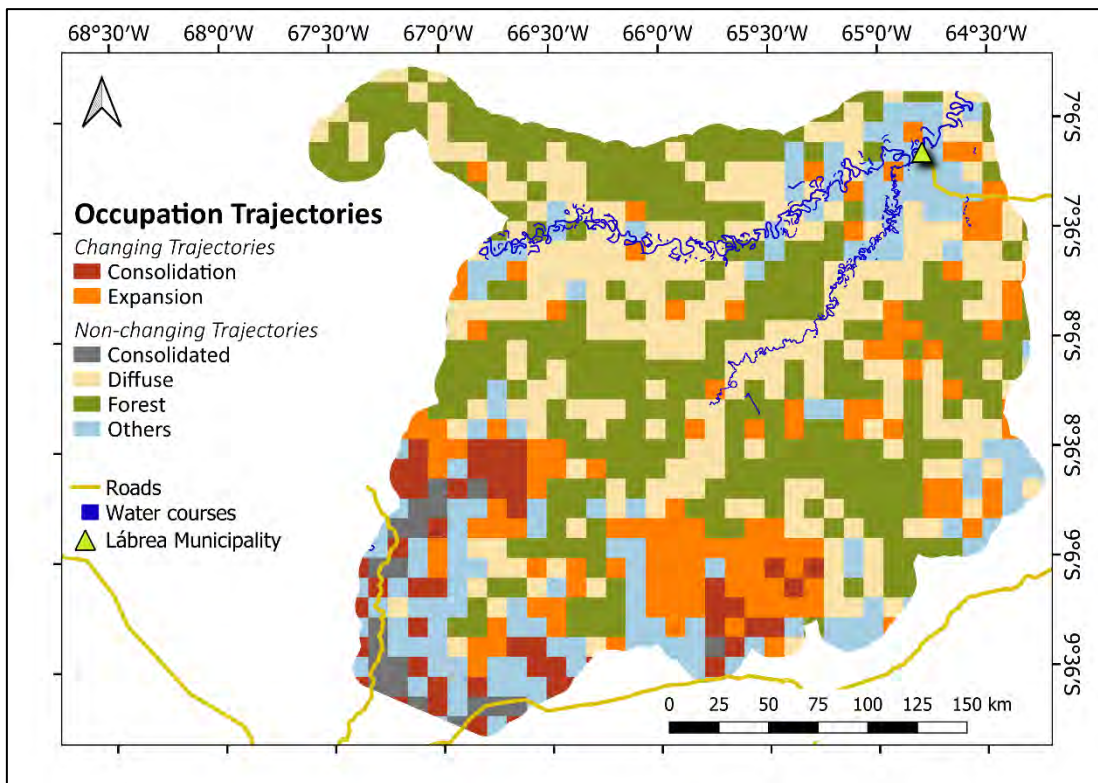
Figure 6. Final map of deforestation trajectories from 2008 to 2021 for the study area
(i.e., the municipality of Lábrea + 10-km buffer). The "others" non-change trajectory is
represented by the fishbone, geometric, linear, and multidirectional patterns.

The non-change trajectories are portrayed by cells that maintained their pattern,
namely "consolidated", "diffuse", and "others" (i.e., cells that maintained linear,
geometric, fishbone, and multidirectional patterns throughout the analysis period). The
"consolidated" non-change trajectory had the lowest percentage of cells (3.6%), but the
deforested area was 17.4% (Table S.2). These cells refer to areas where there was
intense deforestation prior to 2008 and were therefore already consolidated due to the
observed amount of deforestation. The total deforested area in these cells up to 2021
was 170,000 ha.

The highest frequencies observed belong to the diffuse and "others" non-change
trajectories (Figure 6). Cells that maintained the diffuse pattern (without change) over
the years had the highest frequency, representing 41.2% of Lábrea's total cells.
However, as previously mentioned, the diffuse pattern is characterized by areas of initial
occupation by riverine and extractivist communities with limited dynamics, so the
proportion of deforested area was only 1.4%, or 13,600 ha (Table S.2).

Cells classified as "others" comprised 25.8% of the study area (Table S.2). This
non-change trajectory was responsible for 30.8% of deforestation in Lábrea and
corresponded to an estimated area of 300,000 ha in 2021. Of the total cells classified as
"others," an area of 113,000 ha (11.6%) had the geometric deforestation pattern, and
96,000 ha (9.9%) had the multidirectional pattern.

4. Discussion

The patterns and trajectories of deforestation in Lábrea identified by the present
study have similarities in some respects to the occupation dynamics observed for this
region in previous studies. This is the case when comparing the results to a recent study
that used cellular grids with a resolution of 50 × 50 km for the entire Legal Amazon

468 region (Maurano et al., 2019). Similarities can be observed, such as intermediate and
469 advanced deforestation patterns (i.e., geometric and multidirectional, respectively)
470 concentrated in the southern portion of our study area, as well as the presence of the
471 diffuse pattern distributed throughout our study area. However, Maurano et al. (2019)
472 did not detect the consolidated pattern in Lábrea, indicating the loss of certain patterns
473 at coarser scales and, therefore, the importance of analyzing deforestation patterns and
474 trajectories at the municipal level to better understand local dynamics and how
475 deforestation frontiers advance in deforestation hotspots like Lábrea (Saito et al., 2011).
476   The "expansion" and "consolidation" trajectories were concentrated in the
477 southern portion of Lábrea, more specifically in two areas that were also reported by
478 Tomasi (2018): a portion near the Vista Alegre do Abunã district, which is crossed by
479 the secondary roads known as "Boi" and "Jequitibá," and another area near the
480 municipal seat of Boca do Acre, where the Monte Settlement Project (PA) is located
481 (Figures S.2-1 and S.2-2 in Supplementary material). In addition to these two areas,
482 small areas of expansion and consolidation were observed in our analysis near the
483 Mendes Junior secondary road (Figure S.2-3), located where the states of Amazonas,
484 Acre, and Rondônia meet. The intensification of this trajectory occurred mainly in the
485 last four years (2018-2021). The temporal evolution of deforestation patterns and
486 trajectories showed two important features: a large increase in the multidirectional and
487 geometric patterns (classified as an expansion trajectory in Figure 4) near the Boi and
488 Jequitibá secondary roads in 2021, and the presence of cells in consolidation where
489 deforestation is concentrated, followed by cells in expansion in the same area.
490   The dynamics observed in the study area underscore the role of roads as vectors
491 for the expansion of new deforested areas (Fearnside et al., 2009; Souza et al., 2017; dos
492 Santos Junior et al., 2018). Additionally, given the study area's proximity to the Tran-
493 Purus region, it is essential to highlight a few key insights. While the observed
494 evolution of patterns do not directly extend to the Tran-Purus region, it can still have
495 notable impacts (Figures 1 and 4). As is well known, the presence of protected areas
496 acts as the primary driver in reducing the advancement of deforestation into the northern
497 portion of the study area (Tomasi, 2018). However, this situation could change with the
498 degazetting of protected areas, environmental degradation, or the construction of new
499 roads leading to an escalating occupation process (Fearnside et al., 2009; Pack et al.,
500 2016). This last aspect is reinforced by three proposed projects presented by the
501 National Department of Transport Infrastructure (DNIT in Portuguese): the construction
502 of a state highway (AM-175) and two federal highways (BR-230 and BR-317) (DNIT,
503 2021a, 2021b; Figure S.3 in Supplementary material).
504   The geometric deforestation pattern is located near areas with advanced stages of
505 land occupation (i.e., multidirectional and consolidated) and is characteristic of
506 occupations by medium and large landholders, whose main activity is cattle ranching
507 (Gavlak et al., 2011; Saito et al., 2011). The regions in which these patterns are located
508 also coincide with the presence of claims in the Rural Environmental Registry (CAR)
509 that overlap with undesignated public lands (Figure S.4 in Supplementary material).
510 This type of overlap is an indication of land grabbing (Azevedo-Ramos et al., 2020;
511 IPAM, 2021; Moutinho, 2022).
512   Despite the presence of patterns that indicate intermediate and advanced stages
513 of occupation, the diffused deforestation pattern was predominant in Lábrea and was
514 concentrated mainly in the central part of the municipality, near the Purus and Ituxi
515 Rivers. In these areas, the presence of small landholdings and riverside populations with
516 low-impact agro-extractive practices is common, which characterizes the small
517 deforested polygons of the diffuse pattern (Schubart, 1983). Similar patterns were also

518 found by Gavlak (2011) in the Sustainable Forest District (DFS) of Highway BR-163 in
519 western Pará, and by Saito et al. (2011) in parts of the states of Pará, Mato Grosso, and
520 the southern edge of Amazonas.
521   In 2008, the federal government created four conservation units in the northern
522 portion of Lábrea, two extractive reserves (Resex Médio Purus and Ituxi), a national
523 park (PARNA Mapinguari) and a national forest (FLONA do Iquiri) (Figure 1). These
524 were created in the context of the proposed reconstruction of BR-319 connecting Porto
525 Velho to Manaus (Franco, 2011). Since there were no significant changes in the
526 frequency of the diffuse deforestation pattern over time, as well as the proportion of the
527 deforested area that this pattern represented, it is assumed that most of the deforestation
528 observed in the diffuse cells occurred before 2008. This underscores the impact of
529 protected areas in mitigating deforestation, even when they have a sustainable-use
530 designation, such as extractive reserves (areas designated for extraction of rubber,
531 Brazil nuts and other non-timber products), which inherently allow for more permissive
532 activities compared to areas under full protection. Despite this distinction, protected
533 areas play a crucial role in thwarting the progression of patterns associated with early-
534 stage occupations, preventing them from advancing into more advanced stages of
535 occupation and deforestation (Vitel et al., 2009; Soares-Filho et al., 2010; Walker et al.,
536 2020).
537   The linear pattern is associated with early stages of occupation mainly in the
538 vicinity of secondary roads. Depending on the region where they are located, cells with
539 this pattern can easily evolve into more advanced stages of deforestation, acting as a
540 vector for forest loss in previously inaccessible areas. In this study, the proportion of
541 cells classified as linear was small compared to other patterns. These cells were
542 distributed in areas near the municipal headquarters of Lábrea and in settlement
543 projects. It is important to note that the confusion matrices for the analyzed years
544 indicated classification errors between the linear pattern and the fishbone and geometric
545 patterns. These errors were also found by Gavlak (2011) due to the low frequency of
546 this pattern in his study area.
547   Although studies have related the fishbone pattern to the evolution of linear
548 patterns in some areas in the early stages of road construction, such as BR-319 and BR-
549 364 (Sampaio and Costa, 2009; Saito, 2010), this behavior was not so evident in the
550 present study. This may be associated with the stage of occupation in Lábrea, which, in
551 the analyzed years, presented more advanced occupation patterns (i.e., multidirectional
552 and consolidated). In addition, deforestation expansion from secondary roads connected
553 to main roads in the southern portion of the municipality occurred before 2008, with a
554 large portion of the trajectories observed being of the non-change type.
555   The evolution of patterns in existing settlement projects indicates that, until
556 2017, the Monte settlement project (located near the municipal seat of Boca do Acre)
557 displayed a fishbone pattern. By overlaying cells representing deforestation patterns
558 onto settlement boundaries, it became evident that the Gedeão Sustainable Development
559 Project (PDS) also exhibits fishbone patterns, despite being categorized as an
560 "environmentally differentiated" settlement project where actors and deforestation
561 patterns are expected to differ from a traditional settlement project (PA) (Yanai et al.,
562 2017). The presence of fishbone patterns in the initial analysis periods is linked to the
563 more intense occupation process in these settlement projects, particularly in the 2000s
564 (Tomasi, 2018).
565   Our findings reveal a significant intensification of deforestation in recent years
566 in the southern portion of Lábrea, specifically near the Boi and Jequitibá secondary
567 roads. This contrasts with the northern portion of the municipality, where the city of

568 Lábrea is located. The drivers behind the consolidation and expansion of deforestation
569 in this region are diverse, encompassing factors such as the dismantling of
570 environmental policies, increased conflicts in rural areas, weakened environmental
571 enforcement, land grabbing, illegal logging, and proximity to highways (Brito et al.,
572 2019; Ferrante and Fearnside, 2019; Azevedo-Ramos et al., 2020; Vale et al., 2021;
573 Wenzel, 2023).

574   Studies that identify the relationships between occupation dynamics and
575 economic, social, and environmental variables are crucial for defining strategic actions
576 to curb the deforestation that is advancing into forest areas in the municipality of
577 Lábrea. A recent study applying Bayesian techniques has shown that effectiveness of
578 past measures to slow Amazon deforestation depended heavily on the measures being
579 tailored to the types of actors present and to each area's degree of consolidation
580 (Brandão et al., 2023). Future studies should explore the relationship between the
581 observed deforestation patterns and fire occurrence, given their close association (Silva
582 et al., 2021; Dutra et al., 2023). Finally, the current study in the municipality of Lábrea
583 illustrates that these key variables and their trajectories can be quantified through
584 remote sensing. The application of these techniques could contribute to the
585 understanding of deforestation patterns, providing valuable insights for informing
586 political actions aimed at reducing deforestation rates not only within the eight-nation
587 PanAmazonian region, but also in other tropical forest areas globally.

588
589 **5. Conclusions**

590   The dynamics of deforestation in cattle-ranching frontier areas in the
591 municipality of Lábrea show that processes of occupancy and deforestation frontier
592 expansion do not occur uniformly. Identifying different trajectories of change is
593 essential for the development of actions to contain new illegal land occupations and the
594 increase in patterns that contribute most to deforestation, such as the multidirectional
595 and consolidated patterns that indicate advanced stages of occupation. It is also
596 important to focus efforts on areas with the consolidation trajectory, which, despite its
597 lower frequency, accounted for the largest deforested area in the municipality of Lábrea.

598   The areas bordering Lábrea in the neighboring the states of Rondônia and Acre
599 consisted mostly of areas with the consolidation trajectory, which had the highest
600 increase in forest loss over the 2017-2021 period. The growth of this trajectory is
601 mainly related to the increase in the multidirectional pattern (i.e., advanced stage of
602 occupancy). Next to these trajectories, expansion zones were identified that advance
603 from the southern part of Amazonas state into new areas to the north. This is
604 particularly concerning for the vast Trans-Purus region, located to the north and west if
605 Lábrea.

606   The patterns and trajectories of land-use change indicate how and where
607 deforestation occurs and allow identifying the types of actors responsible for this
608 dynamic. This technique can contribute to the development of public policies focused
609 on forest conservation and protection throughout Amazonia and in other tropical
610 regions. It is necessary to strengthen protected areas, which were observed to play an
611 important role in controlling deforestation. Effective measures to control deforestation
612 require tailoring them to the types of actors and to the degree of consolidation of
613 occupation. The techniques developed in this study can facilitate quantifying these
614 factors over wide areas in Amazonia and elsewhere in the tropics.
615

7. References

Agrawal, A.; Brown, D.G.; Sullivan, J.A. 2019. Are global land grabs ticking socio-environmental bombs or just inefficient investments? One Earth, 1, 159–162. https://doi.org/10.1016/J.ONEEAR.2019.10.004.

Alencar, A.; Silvestrini, R.; Gomes, J.; Savian, G. 2022. Amazônia em chamas – O novo e alarmante patamar do desmatamento na Amazônia. Nota técnica n° 9. Brasília, DF, Brazil: Instituto de Pesquisa Ambiental da Amazônia. (https://bit.ly/3YmFdYG). Accessed: 22 July 2022.

Alvares, C.A.; Stape, J.L.; Sentelhas, P.C.; Gonçalves, J.L.M.; Sparovek, G. 2013. Köppen's climate classification map for Brazil. Meteorologische Zeitschrift, 22(6), 711-728. https://doi.org/10.1127/0941-2948/2013/0507.

Antunes, A.F.B.; Lingnau, C. 1997. Uso dos índices de acurácia para avaliação de mapas temáticos obtidos por meio de classificação digital. In: Anais do III Congresso e Feira para Usuário de Geoprocessamento. Curitiba, Paraná, Brazil: Sagres. http://bit.ly/3Zmzqnh.

Arraut, J.M.; Nobre, C.A.; Barbosa, H.M.; Obregon, G.; Marengo, J.A. 2012. Aerial rivers and lakes: Looking at large-scale moisture transport and its relation to Amazonia and to subtropical rainfall in South America. Journal of Climate, 25, 543-556. https://doi.org/10.1175/2011JCLI4189.1.

Assis, L.F.F.G. Ferreira, K.R.; Vinhas, L.; Maurano, L.; Almeida, C.; Carvalho, A.; Rodrigues, J.; Maciel, A.; Camargo, C. 2019. TerraBrasilis: A spatial data analytics infrastructure for large-scale thematic mapping. ISPRS International Journal of Geo-Information, 8, art. 513. https://doi.org/10.3390/ijgi8110513

Assis, T.O.; Escada, M.I.S.; Amaral, S. 2021. Effects of deforestation over the Cerrado landscape: A study in the Bahia frontier. Land, 10(4), art. 352. https://doi.org/10.3390/land10040352.

Azeredo, M.; Monteiro, A.M.V.; Escada, M.I.S.; Ferreira, K.R.; Vinhas, L.; Pinheiro, T.F. 2016. Mineração de trajetórias de mudança de cobertura da terra em estudos de degradação florestal. Revista Brasileira de Cartografia, 68(4), 717–731. https://doi.org/10.14393/rbcv68n4-44278.

Azevedo-Ramos, C. Moutinho, P.; Arruda, V.L.S.; Stabile, M.C.C.; Alencar, A.; Castro, I.; Ribeiro, J.P. 2020. Lawless land in no man's land: The undesignated public forests in the Brazilian Amazon. Land Use Policy, 99, art. 104863. https://doi.org/10.1016/j.landusepol.2020.104863.

Barros, H.S.; Fearnside, P.M. 2019. Soil carbon is decreasing under "undisturbed" Amazonian forest. Soil Science Society of America Journal, 83(6), 1779-1785. http://doi.org/10.2136/sssaj2018.12.0489.

Biastoch, A.; Boning, C.W. 2013. Anthropogenic impact on Agulhas leakage. Geophysical Research Letters, 40, 1138–1143. https://doi.org/10.1002/grl.50243.

666 Brandão, F.; Befani, B.; Soares-Filho, J.; Rajão, R.; Garcia, E. 2023. How to halt
667   deforestation in the Amazon? A Bayesian process-tracing approach. Land Use
668   Policy, 133, art. 106866. https://doi.org/10.1016/j.landusepol.2023.106866.
669 Brito, B.; Barreto, P.; Brandão Jr., A.; Baima, S.; Gomes, P.H. 2019. Stimulus for land
670   grabbing and deforestation in the Brazilian Amazon. Environmental Research
671   Letters, 14(6), art. 064018. https://doi.org/0.1088/1748-9326/ab1e24
672 Coelho, C.A.S., de Oliveira, C.P., Ambrizzi, T. et al. 2016. The 2014 southeast Brazil
673   austral summer drought: regional scale mechanisms and teleconnections. Climate
674   Dynamics. 46, 3737–3752. https://doi.org/10.1007/s00382-015-2800-1.
675 CPT (Comissão Pastoral da Terra). 2021. Conflitos no Campo Brasil 2021: CEDOC
676   Dom Tomás Balduino – CPT. http://bit.ly/3F0rtfo.
677 Cunha, A.P.M.A.; Zeri, M.; Deusdará Leal, K.; Costa, L.; Cuartas, L.A.; Marengo, J.A.;
678   Tomasella, J.; Vieira, R.M.; Barbosa, A.A.; Cunningham, C. et al. 2019. Extreme
679   drought events over Brazil from 2011 to 2019. Atmosphere, 10, art. 642.
680   https://doi.org/10.3390/atmos10110642.
681 Diniz, A.M. 2002. Migração e evolução na fronteira agrícola. In: Anais do XIII
682   Encontro da Associação Brasileira de Estudos Populacionais, Ouro Preto, Minas
683   Gerais, 2002. Campinas, São Paulo, Brazil: Associação Brasileira de Estudos
684   Populacionais. 26 pp.
685 dos Santos Júnior, M.A.; Yanai, A.M.; Sousa Junior, F.O.; de Freitas, I.S.; Pinheiro,
686   H.P.; de Oliveira, A.C.R.; da Silva, F.L.; Graça, P.M.L.A.; Fearnside, P.M. 2018.
687   BR-319 como Propulsora de desmatamento: Simulando o Impacto da Rodovia
688   Manaus-Porto Velho, Instituto de Desenvolvimento Sustentável da Amazônia
689   (IDESAM), Manaus, Amazonas, Brazil. 56 pp. https://bit.ly/3yjpdfe.
690 DNIT (Departamento Nacional de Infraestrutura de Transportes). 2021a. Rodovias
691   Federais. (https://servicos.dnit.gov.br/vgeo/). Accessed: 12 June 2021.
692 DNIT (Departamento Nacional de Infraestrutura de Transportes). 2021b. Rodovias
693   Estaduais. (https://servicos.dnit.gov.br/vgeo/). Accessed: 12 June 2021.
694 Dutra, D.J.; Anderson, L.O.; Fearnside, P.M.; Graça, P.M.L.d.A.; Yanai, A.M.;
695   Dalagnol, R.; Burton, C.; Jones, C.; Betts, R.; Aragão, L.E.O.e.C.d. 2023. Fire
696   dynamics in an emerging deforestation frontier in southwestern Amazonia, Brazil.
697   Fire, 6(2). https://doi.org/10.3390/fire6010002.
698 Fearnside, P.M. 2004. A água de São Paulo e a floresta amazônica. Ciência Hoje,
699   34(203), 63-65. http://philip.inpa.gov.br/publ_livres/2004/S%20PAULO-agua-
700   C%20hoje.pdf
701 Fearnside, P.M. 2015. Rios voadores e a água de São Paulo. Amazônia Real.
702   https://bit.ly/3qykIsY.
703 Fearnside, P.M. 2017. Deforestation of the Brazilian Amazon. In: H. Shugart (ed.)
704   Oxford Research Encyclopedia of Environmental Science. Oxford University
705   Press, New York, USA. https://doi.org/10.1093/acrefore/9780199389414.013.102.
706 Fearnside, P.M. 2018. BR-319 e a destruição da floresta amazônica. Amazônia Real, 19
707   October 2018. (http://bit.ly/3IRS0MX). Accessed: 14 March 2021.
708 Fearnside, P.M. 2021a. Deforestation in Brazilian Amazonia. In: E. Wohl (ed.) Oxford
709   Bibliographies in Environmental Science. New York, USA: Oxford University
710   Press. https://doi.org/10.1093/obo/9780199363445-0064.
711 Fearnside, P.M. 2021b. Lessons from Brazil's São Paulo droughts (commentary).
712   Mongabay, 30 July 2021. https://news.mongabay.com/2021/07/lessons-from-
713   brazils-sao-paulo-droughts-commentary/. Accessed: 14 March 2021.

714 Fearnside, P.M. 2022. Amazon environmental services: Why Brazil's Highway BR-319
715   is so damaging. Ambio, 51, 1367–1370. https://doi.org/10.1007/s13280-022-
716   01718-y.
717 Fearnside, P.M.; Ferrante, L.; Yanai, A.M.; Isaac Júnior, M.A. 2020. Trans-Purus:
718   Brazil's last intact Amazon forest at immediate risk (commentary) Mongabay, 24
719   November 2020. https://bit.ly/3IrTJH5. Accessed: 14 March 2021.
720 Fearnside, P.M.; Graça, P.M.L.A.; Keizer, E.W.H.; Maldonado, F.D.; Barbosa, R.I.;
721   Nogueira, E.M. 2009. Modelagem de desmatamento e emissões de gases de efeito
722   estufa na região sob influência da rodovia Manaus-Porto Velho (BR-319). Revista
723   Brasileira de Meteorologia, 24(2), 208-233. https://doi.org/10.1590/S0102-
724   77862009000200009.
725 Fernandes, V.R.; Cunha, A.P.M.; do Amaral, P.; Luz, A.C.; Leal, K.R.D.; Costa,
726   L.C.O.; Broedel, E.; Alvalá, R.C.S.; Seluchi, M.E.; Marengo, J. 2021. Secas e os
727   impactos na região Sul do Brasil. Revista Brasileira de Climatologia, 28, 561-584.
728   https://doi.org/10.5380/rbclima.v28i0.74717.
729 Ferrante, L.; Fearnside, P.M. 2019. Brazil's new president and 'ruralists' threaten
730   Amazonian's environment, traditional peoples and the global climate.
731   Environmental Conservation, 46, 261-263.
732   https://doi.org/10.1017/S0376892919000213.
733 Franco, M.H.M. 2011. Novas configurações territoriais no Purus indígena e extrativista.
734   In: G.M. dos Santos (ed.) Álbum Purus. Manaus, Amazonas, Brazil: EDUA, vol. 1,
735   pp. 153-166. https://amazonianativa.org.br/2013/10/16/novas-configuracoes-
736   territoriais-no-purus-indigena-e-extrativista/.
737 Gavlak, A.A. 2011. Padrões de Mudança de Cobertura da Terra e Dinâmica
738   Populacional no Distrito Florestal Sustentável da BR-163: População, Espaço e
739   Ambiente. Master's dissertation in remote sensing. São José dos Campos: INPE
740   http://bit.ly/3kM9vX7.
741 Gavlak, A.A.; Escada, M.I.S.; Monteiro, A.M.V. 2011. Dinâmica de padrões de
742   mudança de uso e cobertura da terra na região do Distrito Florestal Sustentável da
743   BR-163. In: Simpósio Brasileiro de Sensoriamento Remoto, 15. (SBSR), Curitiba.
744   São José dos Campos, São Paulo, Brazil: INPE, pp. 6152-6160.
745   http://marte.dpi.inpe.br/col/dpi.inpe.br/marte/2011/06.27.12.54/doc/p1188.pdf
746 Getirana, A.; Libonati, R.; Cataldi, M. 2021. Brazil is in water crisis — It needs a
747   drought plan. Nature, 600, 218-220. https://doi.org/10.1038/d41586-021-03625-w.
748 Hudson, W.D.; Ramm, C.W. 1987. Correct formulation of the Kappa coefficient of
749   agreement. Photogrammetric Engineering and Remote Sensing, 53(4), 421–422.
750   https://www.asprs.org/wp-content/uploads/pers/1987journal/apr/1987_apr_421-
751   422.pdf.
752 IBGE (Instituto Brasileiro de Geografia e Estatística). 2017. Censo Agropecuário 2017 -
753   Resultados definitivos.
754   (https://cidades.ibge.gov.br/brasil/am/labrea/pesquisa/24/76693). Accessed: 7
755   February 2021.
756 IBGE (Instituto Brasileiro de Geografia e Estatística). 2020. Solos.
757   (http://bit.ly/3JdipGm). Accessed: 11 January 2021.
758 IBGE (Instituto Brasileiro de Geografia e Estatística). 2021b. Lábrea.
759   (https://cidades.ibge.gov.br/brasil/am/labrea/panorama). Accessed: 13 August
760   2021.
761 IBGE (Instituto Brasileiro de Geografia e Estatística). 2021a. Malha Municipal.
762   (https://bit.ly/3kQywjU). Accessed: 14 August 2021.

763 ICMBIO (Instituto Chico Mendes de Conservação da Biodiversidade). 2021. Unidades
764   de Conservação. (https://bit.ly/3kQU7bO). Accessed: 15 January 2021.

765 IMAZON (Instituto do Homem e Meio Ambiente da Amazônia). 2022. Desmatamento
766   na Amazônia cresce 29% em 2021 e é o maior dos últimos 10 anos. IMAZON, 17
767   January 2022. (http://bit.ly/3Yom4FC). Accessed: 28 January 2022.

768 InfoAmazonia. 2021. Sul do Amazonas é a nova fronteira do desmatamento na
769   Amazônia, InfoAmazonia, 22 December 2021. (http://bit.ly/3EZxqJu). Accessed:
770   22 July 2022.

771 INPE (Instituto Nacional de Pesquisas Espaciais). 2020. TerraView. São José dos
772   Campos, São Paulo, Brazil: INPE. (http://bit.ly/3JdqACK). Accessed: 2 April
773   2022.

774 INPE (Instituto Nacional de Pesquisas Espaciais). 2021. Desmatamento - Amazônia
775   Legal. INPE, Coordenação Geral de Observação da Terra. Programa de
776   Monitoramento da Amazônia e Demais Biomas. (http://bit.ly/3ZuuFIw). Accessed:
777   9 June 2021.

778 IPAM (Instituto de Pesquisa Ambiental da Amazônia). 2021. Invasão de terras públicas
779   foi a principal causa do desmatamento na Amazônia. IPAM, 22 November 2021.
780   (http://bit.ly/3ZjFoFo). Accessed: 3 January 2022.

781 Körting, T.S.; Fonseca, L.M.G.; Escada, M.I.S.; Silva, F.C.; Silva, M. 2008. GeoDMA
782   – A novel system for spatial data mining. In: ICDMW '08: Proceedings of the 2008
783   IEEE International Conference on Data Mining Workshops, December 2008. Pisa,
784   Italy. pp. 975–978. https://doi.org/10.1109/ICDMW.2008.22.

785 Laurance, W.F.; Cochrane, M.A.; Bergen, S.; Fearnside, P.M.; Delamônica, P.; Barber,
786   C.; D'Angelo, S.; Fernandes, T. 2001. The future of the Brazilian Amazon.
787   Science, 291, 438-439. https://doi.org/10.1126/science.291.5503.438.

788 Marinaro, S.; Sacchi, L.; Gasparri, N.I. 2022. From whom and for what: Deforestation
789   in Dry Chaco from local-urban inhabitants' perceptions. Perspectives in Ecology
790   and Conservation, 20, 141-150. https://doi.org/10.1016/j.pecon.2021.12.003.

791 Maurano, L.E.P.; Escada, M.I.S.; Renno, C.D. 2019. Padrões espaciais de
792   desmatamento e a estimativa da exatidão dos mapas do PRODES para Amazônia
793   Legal Brasileira. Ciência Florestal [Santa Maria], 29(4), 1763-1775.
794   https://doi.org/10.5902/1980509834380.

795 McGarigal, K.; Marks, B.J. 1995. FRAGSTATS: Spatial pattern analysis program for
796   quantifying landscape structure. Washington: United States Department of
797   Agriculture, 132 pp. (Pacific Northwest Research Station General Technical
798   Report PNW-GTR-351). https://www.fs.usda.gov/pnw/pubs/pnw_gtr351.pdf.

799 Mertens B.; Lambin, E.F. 1997. Spatial modeling of deforestation in southern
800   Cameroon. Spatial disaggregation of diverse deforestation processes. Applied
801   Geography, 17(2), 143-162. https://doi.org/10.1016/S0143-6228(97)00032-5.

802 Moutinho, P. 2022. Comissão de Meio Ambiente debate denúncia fraude no Cadastro
803   Ambiental Rural em 25 de maio de 2022. TV Senado. (http://bit.ly/3KZh07D).
804   Accessed: 2 May 2022.

805 NICFI (Norway´s International Climate and Forest Initiative). 2021. NICFI Data
806   Program. https://www.nicfi.no/.

807 Nicolini, M.; Saulo, C.; Torres, J.C.; Salio, P. 2002. Enhanced precipitation over
808   southeastern South America related to low-level jet events during austral warm
809   season. Meteorologica, 27, 59–70.
810   https://ri.conicet.gov.ar/bitstream/handle/11336/148157/CONICET_Digital_Nro.d
811   d6add01-8def-48e5-80f7-250a4f9f98af_A.pdf?sequence=2&isAllowed=y.

812 Nobre, C., Marengo, J., Seluchi, M., Cuartas, L.; Alves, L. 2016. Some characteristics
813   and impacts of the drought and water crisis in southeastern Brazil during 2014 and
814   2015. Journal of Water Resource and Protection, 8, 252-262.
815   https://doi.org/10.4236/jwarp.2016.82022.
816 Nogueira, E.M.; Yanai, A.M.; Fonseca, F.O.R.; Fearnside, P.M. 2015. Carbon stock
817   loss from deforestation through 2013 in Brazilian Amazonia. Global Change
818   Biology 21, 1271–1292. https://doi.org/10.1111/gcb.12798.
819 Oliveira Filho, F.J.B.; Metzger, J.P. 2006. Threshold in landscape structure for three
820   common deforestation patterns in the Brazilian Amazon. Landscape Ecology, 21,
821   1061-1073. https://doi.org/10.1007/s10980-006-6913-0.
822 Pack, S. M.; Ferreira, N.F.; Krithivasan, R.; Murrow, J.; Bernard, E.; Mascia, M. B.
823   2016. Protected area downgrading, downsizing, and degazettement (PADD) in the
824   Amazon. Biological Conservation, 197, 32-39.
825   https://doi.org/10.1016/j.biocon.2016.02.004.
826 Pereira, L.M.; Escada, M.I.; Rennó, C.D. 2007. Análise da evolução do desmatamento
827   em áreas de pequenas, médias e grandes propriedades na região centro-norte de
828   Rondônia, entre 1985 e 2000. Anais do XIII Simpósio Brasileiro de Sensoriamento
829   Remoto, Florianópolis, Brasil, 21-26 abril 2007, INPE, pp. 6905-6912.
830   http://marte.sid.inpe.br/col/dpi.inpe.br/sbsr@80/2006/11.10.12.31/doc/6905-
831   6912.pdf.
832 Pinheiro, T.F.; Escada, M.I.S.; Valeriano, D.M.; Hostert, P.; Gollnow, F.; Müller, H.
833   2016. Forest degradation associated with logging frontier expansion in the
834   Amazon: The BR-163 region in southwestern Pará, Brazil. Earth Interactions, 20,
835   art. 17. https://doi.org/10.1175/EI-D-15-0016.1.
836 Quinlan, J.R. 2017. C5.0: An Informal Tutorial. (https://bit.ly/3ygRYtk). Accessed: 9
837   May 2021.
838 RADAMBRASIL 1978. Folha no. SB 20 Purus: geologia, pedologia, vegetação, e uso
839   potencial da terra. Rio de Janeiro, RJ, Brazil: Departamento Nacional de Produção
840   Mineral. 566 pp. https://biblioteca.ibge.gov.br/index.php/biblioteca-
841   catalogo?view=detalhes&id=23596.
842 Saito, E.A. 2010. Caracterização de Trajetórias de Padrões de Ocupação Humana na
843   Amazônia Legal por Meio de Mineração de Dados.
844   (http://urlib.net/8JMKD3MGP7W/38MM2TL). Master's dissertation in remote
845   sensing, Instituto Nacional de Pesquisas Espaciais, São José dos Campos, SP. 158
846   pp. (https://bit.ly/3YouQn5). Accessed: 12 December 2020.
847 Saito, E.A.; Fonseca, L.M.G.; Escada, M.I.S.; Körting, T.S. 2011. Análise de padrões de
848   desmatamento e trajetória de padrões de ocupação humana na Amazônia usando
849   técnicas de mineração de dados. In: Anais XV Simpósio Brasileiro de
850   Sensoriamento Remoto - SBSR, Curitiba, PR, Brasil, 30 de abril a 05 de maio de
851   2011, São José dos Campos, São Paulo, Brazil: INPE. pp. 2833-2840.
852   https://bit.ly/3ST0eZP.
853 Saito, E.A.; Fonseca, L.M.G.; Escada, M.I.S.; Körting, T.S. 2012. Efeitos da mudança
854   de escala em padrões de desmatamento na Amazônia. Revista Brasileira de
855   Cartografia, 63(3), 401–414. https://doi.org/10.14393/rbcv63n3-43749.
856 Sampaio, L.S.; Costa, R.G.C. 2009. Estradas e suas relações socioambientais. In: Porro,
857   R. (ed.). Alternativa Agroflorestal na Amazônia em Transformação. Brasília, DF,
858   Brazil: Embrapa Informação Tecnológica, 825 pp.
859   https://www.worldagroforestry.org/publication/alternativa-agroflorestal-na-
860   amazonia-em-transformacao.

Santos, J.L.; Yanai, A.M.; Graça, P.M.L.A.; Correia, F.W.S.; Fearnside, P.M. 2023. Amazon deforestation: Simulated impact of Brazil's proposed BR-319 highway project. Environmental Monitoring and Assessment 195(10): art. 1217. https://doi.org/10.1007/s10661-023-11820-7.

Schubart, H.O.R. 1983. Ecologia e utilização das florestas. In: Salati, E. Amazônia: Desenvolvimento, Integração e Ecologia. São Paulo, Brazil: Brasiliense, pp. 101-143.

Silva, C.A.; Santilli, G.; Sano, E.E.; Laneve, G. 2021. Fire occurrences and greenhouse gas emissions from deforestation in the Brazilian Amazon. Remote Sensing, 13(376). https://doi.org/10.3390/rs13030376.

Silva, F.C.; Körting, T.S.; Fonseca, L.M.G.; Escada, M.I.S. 2007. Deforestation pattern characterization in the Brazilian Amazonia. In: Anais do XIII Simpósio Brasileiro de Sensoriamento Remoto, 13. (SBSR), Florianópolis. São José dos Campos, São Paulo, Brazil: INPE. pp. 6207-6214. https://bit.ly/3kS9lgY.

Silva, M.P.S.; Câmara, G.; Escada, M.I.S.; Souza, R.C.M. 2008. Remote-sensing image mining: detecting agents of land-use change in tropical forest areas. International Journal of Remote Sensing, 29(16), 4803-4822. https://doi.org/10.1080/01431160801950634.

Soares-Filho, B.; Moutinho, P.; Nepstad, D.; Anderson, A.; Rodrigues, H.; Garcia, R. 2010. Role of Brazilian Amazon protected areas in climate mitigation. In: 24 (Ed), Proceedings of the National Academy of Sciences USA, 107, 10821–10826. http://www.pnas.org/cgi/doi/10.1073/pnas.0913048107.

Souza, A.A.A.; Pontes, A.N.; Adami, M.; Narvaes, I.S. 2017. A contribuição das estradas e o padrão de desflorestamento e degradação da cobertura florestal no sudoeste paraense. Revista Brasileira de Cartografia, 69(9), 1711-1724. https://doi.org/10.14393/rbcv69n9-44089.

SUDAM (Superintendência do desenvolvimento da Amazônia). 2021. Zona de desenvolvimento sustentável dos Estados do Amazonas, Acre e Rondônia 2021-2027: documento referencial. Belém, Pará: SUDAM. 174 pp. https://irp.cdn-website.com/06e645c5/files/uploaded/amacro.pdf.

Tavares, L.; Cordeiro, L. 2017. Perfil Socioeconômico e Ambiental do Sul do Estado do Amazonas: Subsídios para Análise da Paisagem. Brasília, DF, Brazil: WWF–Brasil. 56 pp. http://bit.ly/3kQVuHu.

Tomasi, A.S. 2018. Grilagem de Terras e Violência Agrária: Criação e Extinção de um Projeto de Reforma Agrária no sul do Amazonas. Campinas, São Paulo, Brazil: Grupo Governança de Terras, Universidade Estadual de Campinas (UNICAMP), 45 pp. https://bit.ly/3mjBYno.

Vale, M.M.; Berenguer, E.; de Menezes, M.A.; de Castro, E.B.V; de Siqueira, L.P.; Portela, R.C.Q. 2021. The COVID-19 pandemic as an opportunity to weaken environmental protection in Brazil. Biological Conservation, 255, art. 108994. https://doi.org/10.1016/j.biocon.2021.108994.

van der Ent, R. J.; Savenije, H. H. G.; Schaefli, B.; Steele-Dunne, S. C. 2010. Origin and fate of atmospheric moisture over continents. Water Resources Research, 46, W09525, https://doi.org/10.1029/2010WR009127.

Vitel, C.S.M.N; Fearnside, P.M.; Graça, P.M.L.A. 2009. Análise da inibição do desmatamento na parte Sudoeste do Arco de desmatamento. In: J.C.N. Epiphanio & L.S. Galvão (Eds.) Anais XIV Simpósio Brasileiro de Sensoriamento Remoto, Natal, Brasil 2009. São José dos Campos, São Paulo, Brazil: Instituto Nacional de Pesquisas Espaciais (INPE), pp. 6377-6384. https://bit.ly/3EUzORx.

910 Walker, W.S.; Gorelik, S.R.; Bazzini, A.; Aragon-Osejo, J.L.; Josse, C.; Meyer, C.; et
911   al. 2020. The role of forest conversion, degradation, and disturbance in the carbon
912   dynamics of Amazon indigenous territories and protected areas. Proceedings of the
913   National Academy of Sciences USA, 117(6), 3015-3025.
914   https://doi.org/10.1073/pnas.1913321117.

915 Wenzel, F. 2023. Os cupins da floresta: Com Bolsonaro, Ministério do Meio Ambiente
916   abriu mão de área na Amazônia onde madeireiros derrubam 45 mil caminhões de
917   árvores. The Intercept Brasil, 17 January 2023. (http://bit.ly/3JGysNy) Accessed:
918   18 January 2023.

919 Yanai, A.M.; Nogueira, E. M.; Graça, P.M.L.A.; Fearnside, P.M. 2017. Deforestation
920   and carbon stocks loss in Brazil's Amazonian settlements. Environmental
921   Management, 59, 393-409. https://doi.org/10.1007/s00267-016-0783-2.

922 Yanai, A.M.; Graça, P.M.L.A.; Escada, M.I.S.; Ziccardi, L.G.; Fearnside, P.M. 2020.
923   Deforestation dynamics in Brazil's Amazonian settlements: Effects on land-tenure
924   concentration. Journal of Environmental Management, 268, art. 110555.
925   https://doi.org/10.1016/j.jenvman.2020.110555.

926 Yanai, A.M.; Graça, P.M.L.A.; Ziccardi, L.G.; Escada, M.I.S.; Fearnside, P.M. 2022.
927   Brazil's Amazonian deforestation: The role of landholdings in undesignated public
928   lands. Regional Environmental Change, 22, art. 30.
929   https://doi.org/10.1007/s10113-022-01897-0.

930 Zemp, D.C., Schleussner, C.-F.; Barbosa, H.M.J.; van der Ent, R.J.; Donges, J.F.;
931   Heinke, J.; Sampaio, G.; Rammig, A. 2014. On the importance of cascading
932   moisture recycling in South America. Atmospheric Chemistry and Physics, 14,
933   13.337–13.359. https://doi.org/10.5194/acp-14-13337-2014.

Supplementary Material

Amazon deforestation: A dangerous future indicated by patterns and trajectories in a hotspot of forest destruction in Brazil

Beatriz Figueiredo Cabral[1], Aurora Miho Yanai[1], Paulo Maurício Lima de Alencastro Graça[1], Maria Isabel Sobral Escada[2], Cláudia Maria de Almeida[2], Philip Martin Fearnside[1]

[1] Instituto Nacional de Pesquisas da Amazônia (INPA), Av. André Araújo n° 2936, CEP 69067-375, Manaus, Amazonas, Brazil, beatriz.figueiredocabral@gmail.com; yanai@inpa.gov.br pmlag@inpa.gov.br; pmfearn@inpa.gov.br
[2] Instituto Nacional de Pesquisas Espaciais (INPE), Av. dos Astronautas, 1758, CEP 12227-010, São José dos Campos, São Paulo, Brazil, isabel.escada@inpe.br; claudia.almeida@inpe.br

Table S.1. Explanation of Landscape Metrics-Based features. (Adapted from McGarigal and Marks, 1995)

Name	Description	Formula
AWMSI	The Area-Weighted Mean Shape Index (AWMSI) is the ratio of the perimeter to the square root of the area, weighted by the patch area, so that larger patches carry more weight than smaller ones, with AWMSI ≥ 1. AWMSI = 1 if all patches are circular or rectangular. This index increases as the complexity of polygons rises, meaning that it increases as shapes become more irregular.	$AWMSI = \sum_{j=1}^{n} \left[\frac{p_j}{2\sqrt{\pi \times a_j}} \times \frac{a_j}{\sum_{j=1}^{n} a_j} \right]$
AWMPDF	Area-Weighted Mean Patch Fractal (AWMPFDF) stands for the fractal dimension of the patch, weighted by the patch area in the landscape. $1 \leq$ AWMPFD ≤ 2, measures the irregularity or complexity of the patch shape. AWMPFD approaches 1 for patches with simpler shapes, such as circles or rectangles, and approaches 2 when patches have a more complex shape.	$AWMPFD = \sum_{j=1}^{n} \left[\frac{2 \times \ln p_j}{\ln a_j} \times \frac{a_j}{\sum_{j=1}^{n} a_{ij}} \right]$
BIA	BIA stands for Biggest Intersection Area of the class in the landscape.	-
CA	Class Area (CA) is a measure of landscape composition represented by the sum of the areas of all fragments of a specific class in hectares (ha). CA > 0. The CA value approaches 0 when there are few patches of the class in the landscape.	$CA = \sum_{j=1}^{n} a_j$

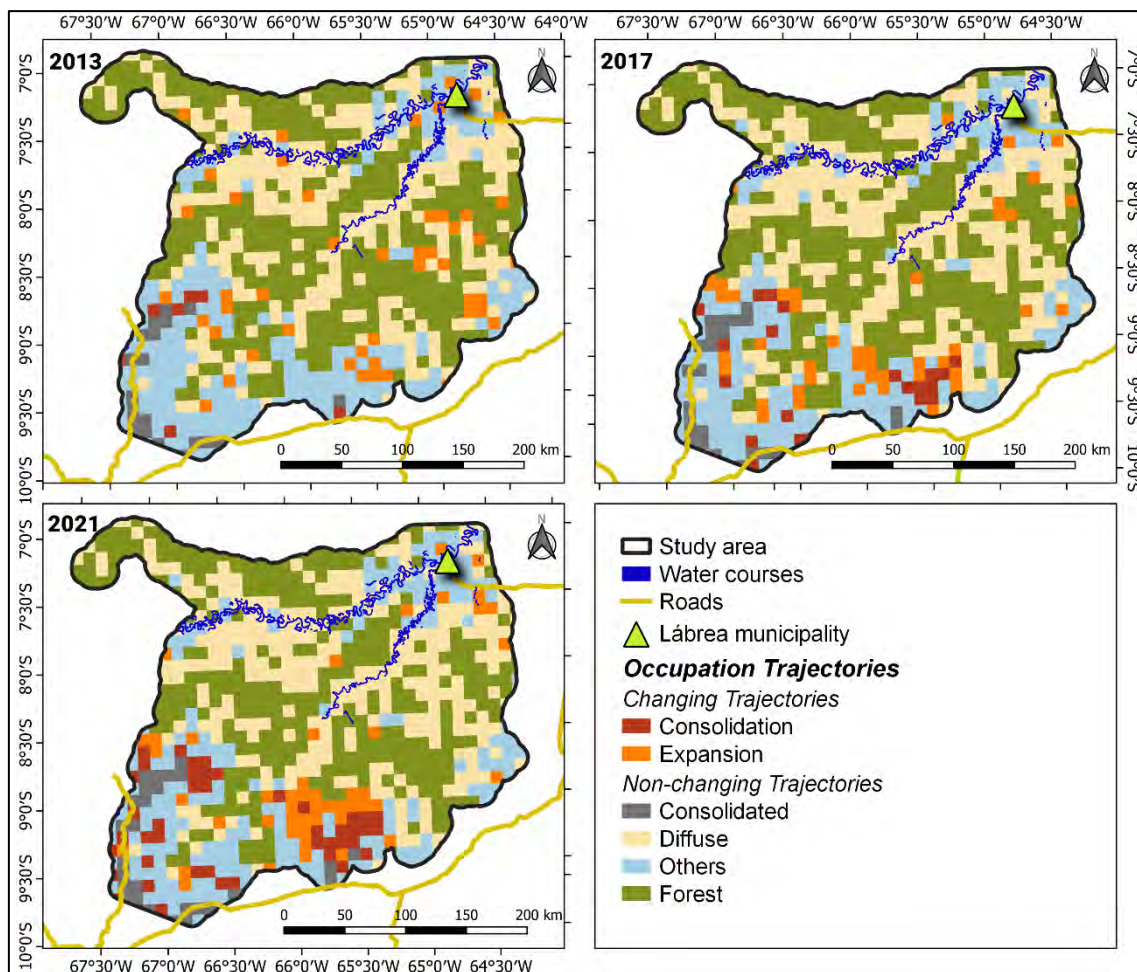| LSI	The Landscape Shape Index (LSI) measures the shape complexity of patches, with LSI ≥ 1, with no set limit. LSI = 1 when the landscape consists of a single patch with a circular or rectangular shape.	$LSI = \frac{\sum_{j=1}^{n} e_j}{2\sqrt{\pi \times A}}$
PD	PD stands for Patch Density, which equals the number of patches in the landscape divided by total landscape area (m²), multiplied by 10,000 and 100 (to convert to 100 hectares). Note, PD does not include background patches or patches in the landscape border, if present. However, total landscape area (A) includes any internal background present.	$PD = \frac{n}{A} \times 10000 \times 100$
PR	PR stands for Patch Richness, which equals the number of different patch types (classes) present within the landscape boundary.	$PR = m$
TABO	TABO stands for the Total Area of the Biggest Object that intersects the landscape.	-

Figure S.1. Maps of the evolution of occupation trajectories in the study area for the periods 2008 to 2013, 2013 to 2017, and 2017 to 2021.

Table S.2. Percentage of deforested cells and total deforested area (in hectares) for each deforestation trajectory from 2008 to 2021 in the study area.

| Deforestation trajectory	Percentage of cells (%)	Deforested area (ha)	Percentage of total deforested area (%)
Consolidation	8.2%	302,297.19	30.8%
Expansion	21.2%	190,824.69	19.6%
Consolidated	3.6%	170,081.82	17.4%
Diffuse	41.2%	13,609.84	1.4%
Others			
Fishbone	3.8%	59,238.17	6.0%
Geometric	5.6%	113,078.94	11.6%
Linear	13.6%	31,718.55	3.3%
Multidirectional	2.8%	96,376.84	9.9%
Subtotal	25.8%	300,412.50	30.8%
TOTAL	**100%**	**977,226.04**	**100%**
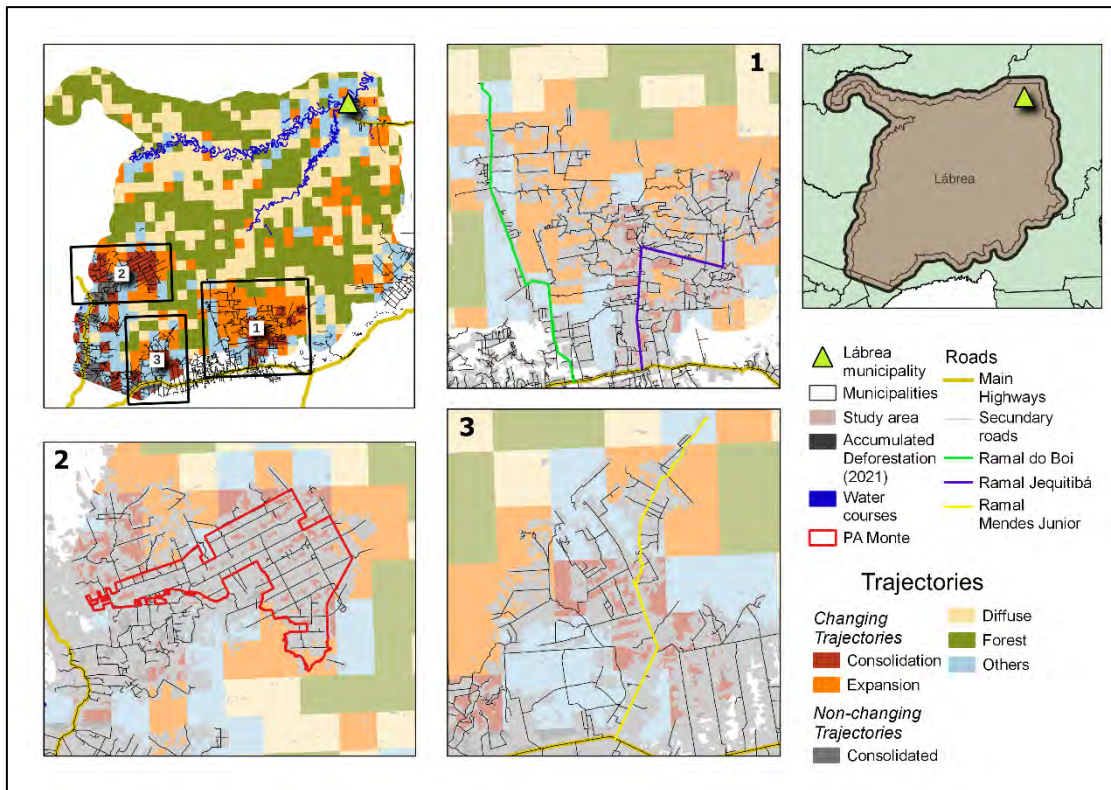
Figure S.2. Areas with advance of the "consolidation" and "expansion" change trajectories for the study area (i.e., the municipality of Lábrea + 10-km buffer) from 2008 to 2021.
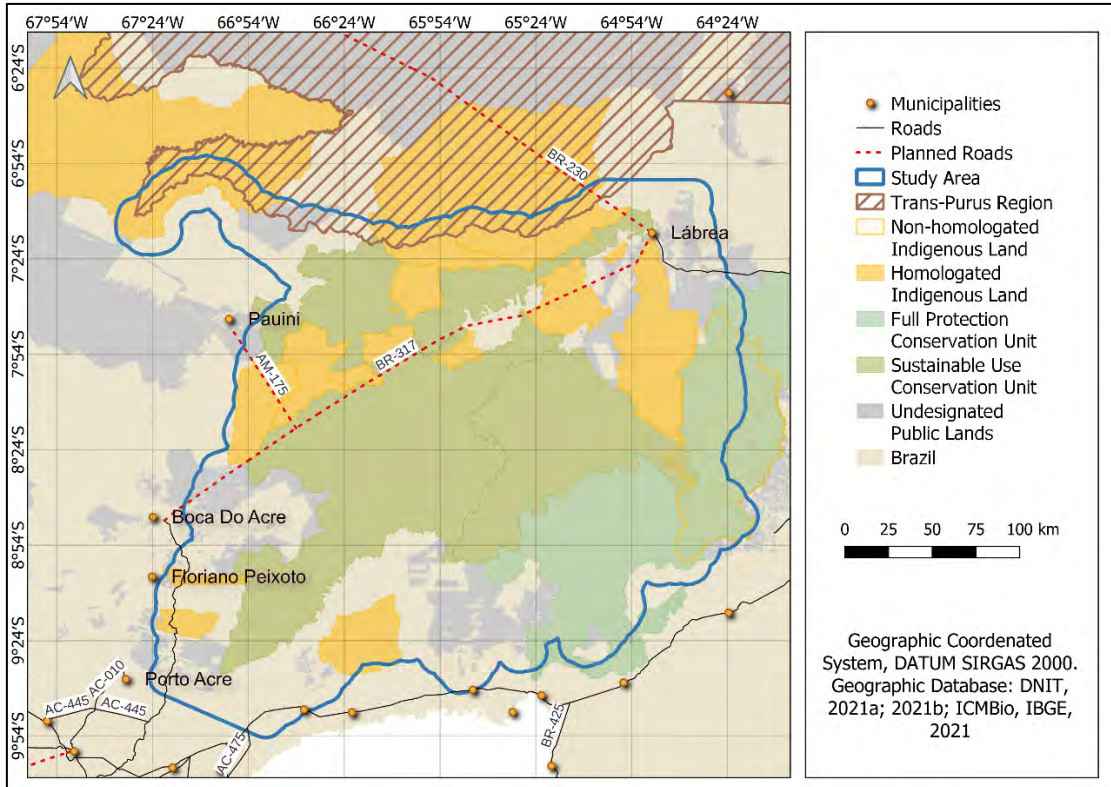

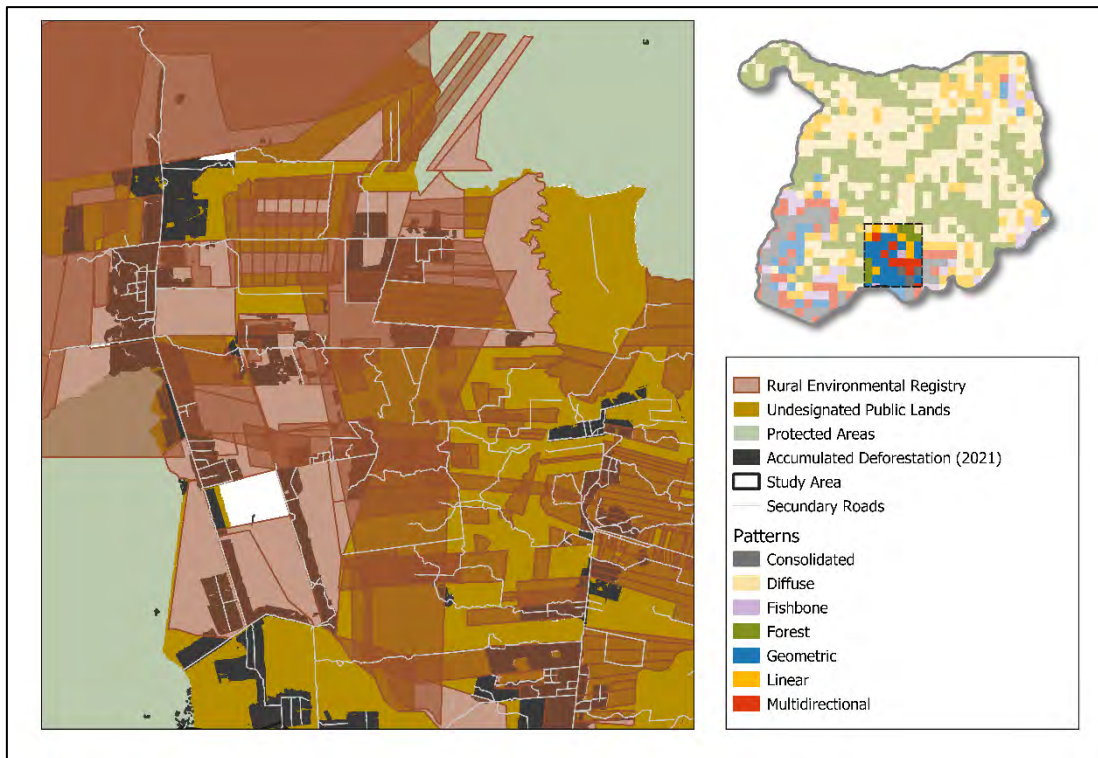**Figure S.3.** Map of planned state and federal highways for the municipality of Lábrea, Amazonas.

Figure S.4. Rural Environmental Registry (CAR) claims overlapping undesignated public lands in 2021, showing concentrations of the geometric deforestation pattern.

Reference

McGarigal, K.; Marks, B.J. 1995. FRAGSTATS: Spatial pattern analysis program for quantifying landscape structure. Washington: United States Department of Agriculture, 132 pp. (Pacific Northwest Research Station General Technical Report PNW-GTR-351). https://www.fs.usda.gov/pnw/pubs/pnw_gtr351.pdf